Optical Near-field Interaction between Neighbouring Micro/Nano-Particles

Zeng Bo Wang[1,*], Wei Guo[1,2], Boris Luk'yanchuk[3], David. J. Whitehead[1], Lin. Li[1], Zhu. Liu[2]

[1]*Laser Processing Research Centre, School of Mechanical, Aerospace and Civil Engineering, University of Manchester, Sackville Street, Manchester, M60 1QD, UK*
[2]*Corrosion and Protection Centre, School of Materials, University of Manchester, The Mill, Manchester M60 1QD, UK*
[3]*Data Storage Institute, DSI Building, 5 Engineering Drive 1, Singapore 117608, Republic of Singapore*

Parallel surface nanopatterning by the enhanced optical near-field under small transparent particles has attracted great attention in recent years. The technique offers great versatility for producing nano-features on the sample surface based on the near-field ablation, etching, deposition and surface modification. Theoretical investigation of the field distribution is generally based on single particle models, e.g. Mie theory or particle-on-surface theory, in which the field interactions between the neighbouring particles have not been well explored. In this paper, the electromagnetic field distribution in the different particle array systems is simulated. Both mono-layered and multiple-layered particle aggregations are addressed. The energy flux between the neighbouring particles in a mono-layered system reveals the existence of energy flowing from central particles to edged particles. The influence of the surrounding medium on the optical near-field interactions in a multi-layered system is also investigated.

DOI: 10.2961/jlmn.2008.01.0004
Keywords: Near-field effects, near-field interaction, coupling, energy flux, surface nanopatterning

1. Introduction

Laser-induced surface nanopatterning has become increasingly important due to the rapid development of nanoelectronics, nanophotonics, super-resolution optical lithography, ultrahigh density optical data storage and biomedical devices [1]. Due to the optical diffraction limit for freely propagating photons, light cannot be confined to a lateral dimension smaller than roughly one half of wavelength in the far-field in free space [2]. In order to overcome this barrier, near-field optics (NFO) , or nano-optics, has attracted much attention in recent years. NFO deals with optical phenomena where evanescent waves become significant. This occurs when the sizes of the scattering objects are of the order of the incident wavelength or smaller [3]. Strong evanescent waves are excited preferentially (though not exclusively) at the boundary of two different media and decay rapidly away from the interface. It may have a dominant role over freely propagating photons in the near-field region of the scattering objects. So far, several near-field patterning techniques exist: near-field scanning optical microscope (NSOM) patterning [4-6]; laser-assisted AFM/STM-tip patterning [7-10]; contacting particle-lens array (CPLA) patterning [11-15]; and plasmonic lithography (PL) [16, 17]. In NSOM and AFM/STM systems, expensive and sophisticated hardware systems are used to control the near-field distance for surface nanopatterning. In addition the throughput is too low to be used in an industrial environment, as they are serial writing techniques. The CPLA technique employs a regular two-dimensional (2D) ordered array of small particles ranging from several tens of nanometer to several tens of micrometer as lens array, which converts a laser beam into a multiplicity of enhanced optical spots in parallel at focus. The CPLA is, therefore, a high-speed parallel processing technique which permits single-step patterning of thousands of holes/cones on the surface with a few laser shots. For the successful implementation of the CPLA technique, a theoretical understanding by the modeling of the localized field distribution in the particle array system is essential. However, most of previous theoretical investigation was generally carried out based on the single particle models, e.g. Mie theory [18] or particle-on-surface theory [19], in which the field interactions between the neighbouring particles have not been well explored. In this paper, the EM field distribution in the different particle array systems is simulated, incorporating both mono-layered and multiple-layered particle aggregations. We also study the influence of the surrounding medium on the optical near-field interactions in a multi-layered system.

2. The Finite Integral Technique (FIT) and simulations

Analytical solution of multiple particle interaction is not trivial, and we seek numerical solution of the problem in this paper. There are several methods for numerically solving electromagnetic problems for an arbitrary geometry. Examples are the multiple multi-pole (MMP) technique [20], the Green's function method [21], the finite difference time domain (FDTD) technique [22] and Finite Integral Technique (FIT) [23], all of which have been applied to solving problems in near-field optics (NFO). The FIT technique, proposed by Weiland, provides a universal spatial discretization scheme, applicable to various electromagnetic problems, ranging from static field calculations to high frequency applications in time or frequency domain.

*) Author to whom correspondence should be addressed;
electronic mail: zengbo.wang@gmail.com

Unlike most numerical methods, FIT discretizes the Maxwell's equation in an integral form rather than the differential ones. In the case of Cartesian grids, the FIT formulation can be rewritten in time domain to yield standard FDTD methods. While in the case of triangular grids, the FIT has tight links with FEM methods formulated in Whitney forms [24]. In this paper, a commercial FIT software package (CST Microwave Studio 2006 [25]) was used. Within a series of tests, we found that CST works well for transparent particles in Cartesian grids system (FDTD module) while a better accuracy can be achieved for plasmonic particles in triangular grids system (FEM module). In present paper, we have chosen to use FDTD module in CST since it can provide faster speed than FEM module for the relatively large particle (1.0 μm) as investigated in the paper. Meanwhile, the FDTD module can also provide complete spectral response of the system in a single computational run. The FDTD algorithm consists of discretizing the Maxwell equations on a 3D-grid and then, starting from a given initial condition, marching a set of iterative relations forward in time. Upon choosing a suitably refined computational grid (the maximum grid length was chosen as wavelength/10 in the paper), the corresponding numerical solution gives an accurate representation of the dynamics of the electromagnetic field. At the boundary of the computational domain, a perfectly matched layer (PML) open boundary condition was applied for all the boundaries (numerical reflection coefficient < 0.01% with a typical four-layered PML). The domain size depends on particle number and its arrangement form as well as the surrounding space size. We fixed the surrounding space size to be 250 nm in all directions. For a 7-particles system as shown later in Fig.1, the mesh cells reach a number of 1,362,102. We set the simulation converges at a energy level of -80 dB which means the solver stops at the moment when the total energy within the calculation domain decays to 10^{-8} of the incident pulse energy. In the following, theoretical studies including both the particle interaction within monolayer and interaction between multi-layered particles are presented. In all modeling, the particle was considered uniform in size with a diameter of 1.0 μm, and a refractive index of 1.51.

In our verification experiment (Fig. 3 below), a KrF excimer laser (Lambda Physik LPX50) was used as the light source ($\lambda = 248$ nm, $\tau = 23$ ns and repetition rate 1 Hz). The sample was a 100 nm-thick eutectic GeSbTe film coated on a polycarbonate substrate. Monodisperse 1.0 μm spherical silica (SiO_2, Duke Scientific) particles were diluted with de-ionized water and applied to the film surface. After water evaporation, a hexagonally closed-packed monolayer was formed on the surface by a self-assembly process. The sample was processed and characterized by field-emission gun electron microscopy (FE-SEM; Hitachi S-4100).

3. Results and Discussions

3.1 Monolayer particle interaction

In experiments, the monolayer particle array is in hexagonal form. The quality over a large surface area depends on many factors such as surface roughness, wetability, solution concentration and temperature. The array was generally observed as a multi-domain arrangement. At the edge region of the array, particles can be arranged in a random form in which one particle can be surrounded by different numbers of particles. Although it could only affect small portion of the patterning domain in a large area application, the importance of studying the coupling effects become obvious when the techniques was used for selectively patterning of particular site where only a small number of particles were used.

Figure 1 shows the intensity field distribution, defined as z-component of the Poynting vector $I = S_z$ which represents the energy flowing into the substrate [26], under particles arranged in different forms: (a) single particle; (b) 3-particles in line; (c) 7-particles in hexagonal form; and (d) an infinite number of particles in hexagonal form. It is observed that the field enhancement factor under the central particle (sitting at $x = 0$ position) decreases with the number of particles surrounding it. The particles on the edge produce higher intensity field underneath them, compared to the central particle in a line or to an isolated particle. When a particle has six surrounding particles as in Fig. 1 (c), the field enhancement under the central particle is around 43, which is clearly below the enhancement of 54 for an

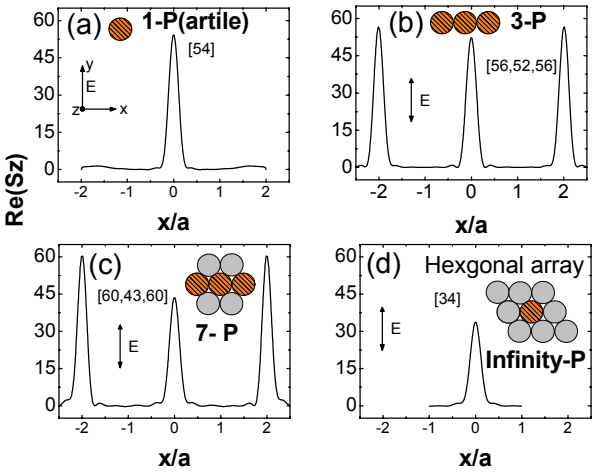

Fig.1 Intensity field distribution under mono-layered particles arranged in different forms: (a) single particle; (b) 3-particles in line; (c) 7-particles in hexagonal form; and (d) an infinite number of particles in hexagonal form. The plot shows the z-component of the Poynting field distribution under the particles marked with line patterns.

isolated particle as in Fig. 1 (a). By contrast, the particles at the edges give an enhancement of 60 which is higher than that of an isolated particle. The peak difference between the central and edged particles in this 7-particle system (Fig. 1c) reaches $\Delta I_{(central-edge)} = 17$ (40% decrease in percentage), which is higher than the peak difference in the 3-sphere system (Fig. 1b) where $\Delta I_{(central-edge)} = 4$ (8% difference). For a perfect hexagonal array system, the enhancement under each particle is 34 (Fig. 1d) which is lower than the value of central particle in all the other three cases (Fig. 1a, 1b, 1c). At the edge of a well-order hexago-

nal array, the peak difference between central and edged particles was found to be $\Delta I_{(central-edge)} \approx 20$ (60% difference). Depending on these peak difference, one can expect some immediate effect that haven't been noticed in CPLA/laser cleaning community, i.e., the threshold for nanopatterning/ laser cleaning could be very different for particles arranged in different forms. According to our findings, we can control the removal sequence of particles when laser fluence increases gradually from low to high values if the sample is processed by a single pulse. First, particles at the large array edge will be removed. This is followed by particles at the array edge, isolated particle and particles within the central region of the array. In the case where multiple laser pulses are used, the area of a particle array shrinks after each pulse due to the removal of particles at edges. New edges are formed after each pulse. The process can be repeated until the array has shrunk to a small number of particles. This can be explained by a process transition from the case of Fig. 1 (d) to (c), to (b) and finally to (a).

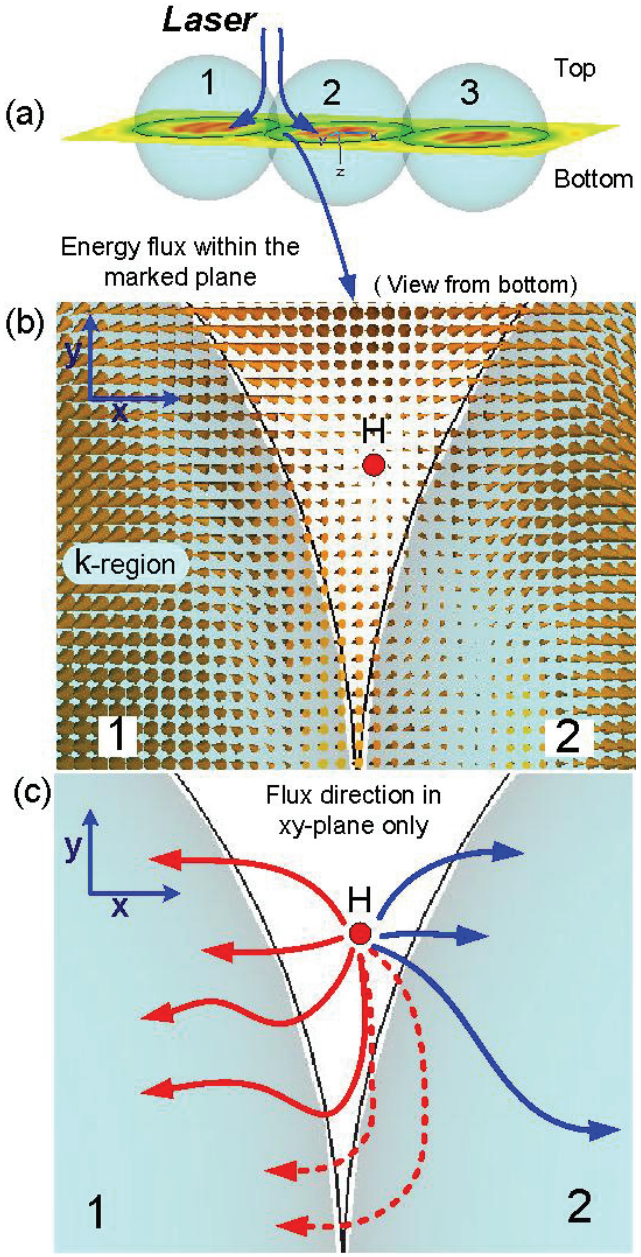

Fig.2 Simulated energy flow within the plane across monolayered particle centers in a 3-sphere system. It was presented with arrows in (b) near the contacting region of sphere 1 and 2. The direction of the flow within the plane is schematically drawn in (c).

To understand why the central peaks increase and edge peaks drop, the energy flux within the contacting plane of neighbouring particles, i.e. in the plane across particle centers, was investigated. Figure 2 shows the simulated energy flow within the plane across particle centers in a lined 3-sphere system. The laser beam was considered to be incident from the top side and the plot in Fig. 2(b) shows the vector plot of Poynting flux viewed from the bottom side in Fig. 2(a). As can be seen in Fig. 2(b), the flux in the k-region (central part of each sphere) has a major component in *z*-direction, indicating that energy flows from the top of the particle to the bottom. In the neighbouring region of particle 1 and 2 (region near H-point), the fluxes become complicated as a singular point H arises in the investigated plane. This means the laser energy (coming from the top as shown in Fig. 2a) passing through the gap regions will be redirected toward both particle 1 and particle 2, as shown by the solid lines in Fig. 2(c). Importantly, one can see some fluxes going from H to particle 2 will flow back to particle 1 (dashed lines in Fig. 2c). This immediately tells why the particles at edges can produce higher enhanced field under them than central particles. In a perfect large-area hexagonal array system (Fig. 2d), Bloch wave modes can be excited which could make the coupling between neighbouring particles even stronger [27], leading to a higher peak difference between central and edged particles.

Figure 3 shows the SEM image of nanodents near the edge region, ablated by the pulsed laser irradiation through a self-assembled particle array. As mentioned above, the field enhancement peak difference between the edge and central particles can reach $\Delta I_{(central-edge)} \approx 20$ in this case. As it can be seen, nanodents were formed throughout the region and the ones near the array edges (row 1 and 2) are deeper because of the higher enhancement field under the particles at the array edges.

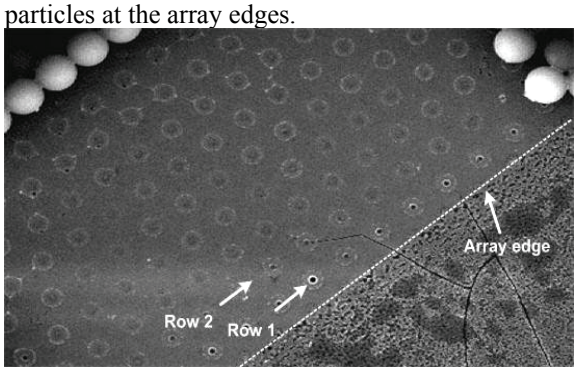

Fig. 3 SEM image of ablated nano-features near the edge of a well-ordered hexagonal particle array. Central holes only appear at positions under the particles at the edge rows 1 and 2.

3.2 Multiple layer particle interaction

In the conventional CPLA technique, it is generally required that the particle array should be in mono-layered form. Multi-layered particles have never been applied in CPLA technique. This is due to the near-field focusing nature of each particle, i.e. the localized laser energy under each particle cannot be efficiently coupled to the underlying layer. To demonstrate this, let us consider a 3-layered hexagonal system (pyramid-like cluster of 11 particles) as shown in Fig. 4(a), in this configuration the distance between the particle centre of layer 3 and layer 1 can be found as:

$$d_{31} = (2.\sqrt{8/3}. - 2).\ r \approx 633 \text{ nm}, \qquad (1)$$

where r is the particle radius with $r = 500$ nm. When the surrounding medium is air or vacuum ($n_m = 1$), one can see from Fig. 4(b)-1 that the focus under the top layer particle is highly localized and confined in a small focal region with a distance $d \le 100$ nm from the bottom of layer 3 particle (see the dashed circle in Fig. 4b-1)[I]. It is clear that in this case there is no significant energy coupling between

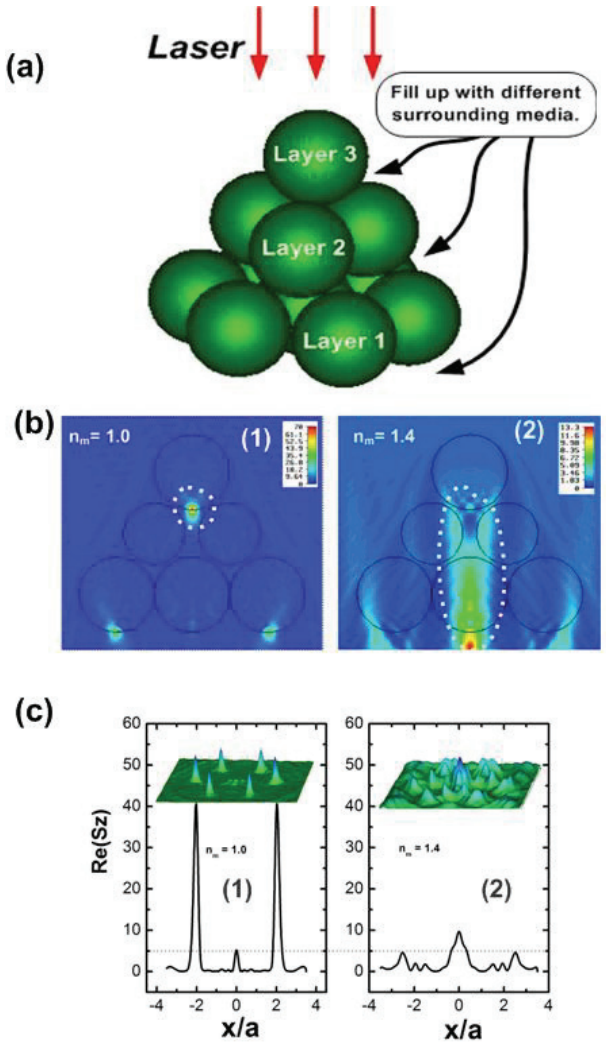

Fig. 4 Optical near-field interaction between multi-layered spheres immersed in different surrounding medium with n = 1.0 (air) and n = 1.4. Both field distribution in (b) cross-section plane and (c) plane under layer 1 particles was shown.

[I] The centers of the layer 2 spheres are not in the same plane with those of layer 1 and 3 spheres, making it looks smaller.

layer 3 and layer 1. As a result, the field peak under the central particle of layer 1 is only ~5 (Fig. 4c-1) which is much smaller than the peak value of 43 in mono-layer system as in Fig. 1(c). To increase the coupling effect between particles in different layers, we propose here to use a different surrounding medium to tune the near-field focal length of the particle. In our modeling, the refractive index of the surrounding medium was changed from $n_m = 1.0$ to $n_m = 1.4$. The corresponding results are shown in Fig. 4b-2 and Fig. 4c-2. Interestingly, one can see from these figures the focal length of the top layer particle has been extended significantly. The layer 1 particle is almost within the focus region of layer 3 particle. At the bottom of layer 1 particle, the central particle peak has increased to around 10, as shown in Fig. 4c-2. The enhancement factor could be further increased when a substrate is present in the system [28]. As a result, multi-layered particle array could be applied in CPLA technique for surface nanopatterning. It should be noted that there is a trade-off between the inter-layer coupling and reflective index selection of the medium: a medium with a too high refractive index could lead to multiple interference modes, which may raise complexity in surface nanopatterning. Additionally, inter-layer coupling could also be enhanced by altering the sphere size or laser wavelength.

4. Conclusions

The optical near-field interaction between neighbouring particles have been investigated. In a mono-layered system, the near-fields under the particles at the edge of particle array can produce a higher enhancement factor due to the in-plane coupling of energy from central particles to edged particles. In multi-layered system, field coupling between different layers is weak in the air environment. However, a higher refractive index medium was helpful in increasing the coupling effect between the different layers of particle array. It is possible to use multi-layered particle array for surface nanopatterning by depositing an appropriate surrounding medium.

Acknowledgments

This work was conducted by the Northwest Laser Engineering Consortium (NWLEC), a collaborative project between the Universities of Liverpool and Manchester, funded by the Northwest Development Agency (NWDA) of the United Kingdom. More information can be found at www.nwlec.org.uk.

References

[1] L. Novotny and B. Hecht, *Principles of Nano-Optics*. 2006, Cambridge: Cambridge University Press.

[2] E. Abbe, *Beitrage zur Theorie des Mikroskops und der mikroskopischen Wahrnehmung.* Archiv Microskop. Anat., 1873. **9**: p. 413.

[3] C. Girard and A. Dereux, *Near-field optics theories.* Rep. Prog. Phys., 1996. **59**: p. 657-699.

[4] E. Betzig, J.K. Trautman, R. Wolfe, E.M. Gyorgy, P.L. Finn, M.H. Kryder, and C.-H. Change, *Near field magneto-optics and high density data storage.* Appl. Phys. Lett., 1992. **61**(2): p. 142-144.

[5] R. Riehn, A. Charas, J. Morgado, and F. Cacialli, *Near-field optical lithography of a conjugated polymer.* Appl. Phys. Lett., 2003. **82**(4): p. 526-528.

[6] G. Wysocki, J. Heitz, and D. Bauerle, *Near-field optical nanopatterning of crystalline silicon.* Appl. Phys. Lett., 2004. **84**(12): p. 2025-2027.

[7] J. Boneberg, H.-J. Münzer, M. Tresp, M. Ochmann, and P. Leiderer, *The mechanism of nanostructuring upon nanosecond laser irradiation of a STM tip.* Appl. Phys. A, 1998. **67**(4): p. 381 - 384.

[8] K. Dickmann, J. Jersch, and F. Demming, *Focusing of laser radiation in the near-field of a tip (FOLANT) for applications in nanostructuring.* Surface and Interface Analysis, 1997. **25**(7-8): p. 500-504.

[9] J. Jersch and K. Dickmann, *Nanostructure fabrication using laser field enhancement in the near field of a scanning tunneling microscope tip.* App. Phys. Lett., 1996. **68**: p. 868.

[10] Y.F. Lu, Z.H. Mai, Y.W. Zheng, and W.D. Song, *Nanostructure fabrication using pulsed lasers in combination with a scanning tunneling microscope: Mechanism investigation.* Appl. Phys. Lett., 2000. **76**(9): p. 1200-1202.

[11] S.M. Huang, M.H. Hong, B. Lukiyanchuk, and T.C. Chong, *Nanostructures fabricated on metal surfaces assisted by laser with optical near-field effects.* Appl. Phys. A, 2003. **77**(2): p. 293-295.

[12] Z.B. Wang, M.H. Hong, B.S.Luk'yanchuk, Y.Lin, Q.F. Wang, and T.C. Chong, *Angle effect in laser nanopatterning with particle-mask.* J. Appl. Phys., 2004. **96**: p. 6845-6850.

[13] R. Piparia, E.W. Rothe, and R.J. Baird, *Nanobumps on silicon created with polystyrene spheres and 248 or 308 nm laser pulses.* Appl. Phys. Lett., 2006. **89**(22): p. 223113.

[14] G. Wysocki, R. Denk, K. Piglmayer, N. Arnold, and D. Bauerle, *Single-step fabrication of silicon-cone arrays.* Appl. Phys. Lett., 2003. **82**(5): p. 692-693.

[15] M. Mosbacher, H.J. Munzer, J. Zimmermann, J. Solis, J. Boneberg, and P. Leiderer, *Optical field enhancement effects in laser-assisted particle removal.* Appl. Phys. A, 2001. **72**(1): p. 41-44.

[16] Z.Liu, Q. Wei, and X. Zhang, *Surface Plasmon Interference Nanolithography.* Nano Lett., 2005. **5**(5): p. 957-961.

[17] W. Srituravanich, S. Durant, H. Lee, C. Sun, and X. Zhang, *Deep subwavelength nanolithography using localized surface plasmons on planar silver mask.* J. Vac. Sci. Technol. B 2005. **23**(6): p. 2636-2639.

[18] G. Mie, *Beiträge zur Optik trüber Medien, speziell kolloidaler Metallösungen.* Ann. Phys. (Leipzig), 1908. **25**: p. 377-445.

[19] P.A. Bobbert and J. Vlieger, *Light scattering by a sphere on a substrate.* Physica, 1986. **137A**: p. 209-242.

[20] C. Hafner, *The Generalized Multiple Multipole Technique for Computational Electromagnetics*. 1990, Boston: Artech.

[21] O.J.F. Martin, C. Girard, and A. Dereux, *Generalized Field Propagator for Electromagnetic Scattering and Light Confinement.* Phys. Rev. Lett., 1995. **74**: p. 526.

[22] A. Taflove, ed. *Computational Electrodynamics: The Finite-Difference Time-Domain Method*. 3rd ed. 2005, Artech House.

[23] T. Weiland, *Time Domain Electromagnetic Field Computation with Finite Difference Methods.* International Journal of Numerical Modelling, 1996. **9**: p. 295-319.

[24] U.V. Rienen, *Numerical Methods in Computational Electrodynamics; Linear Systems in Practical Applications*. 2001, Berlin: Springer.

[25] *Computer Simulation Technology : CST Microwave Studio (http://www.cst.com); Remote license access provided by one of the author B.S. Lukiyanchuk in DSI, Singapore*. 2006.

[26] Z.B. Wang, M.H. Hong, B.S. Luk`yanchuk, S.M. Huang, Q.F. Wang, L.P. Shi, and T.C. Chong, *Parallel nanostructuring of GeSbTe film with particle-mask.* Appl. Phys. A. , 2004: p. 1603-1606.

[27] J.D. Joannopoulos, R.D. Meade, and J.N. Winn, *Photonic crystals: Molding the flow of light*. 1995, Princeton: Princeton University Press.

[28] Z.B. Wang, *Ph.D thesis: Optical resonance and near field effects: small particles under laser irradiation*. 2005, National University of Singapore: Singapore.

(Received: April 24, 2007, Accepted: November 7, 2007)